Drought variation of western Chinese Loess Plateau since 1568 and its linkages with droughts in western North America

Keyan Fang[1,2,3*], Zhengtang Guo[3,4], Deliang Chen[2], Hans W. Linderholm[2], Jinbao Li[5], Feifei Zhou[1], Guoyang Guo[1], Zhipeng Dong[1], Yingjun Li[1]

1. Institute of Geography, Key Laboratory of Humid Subtropical Eco-geographical Process (Ministry of Education), College of Geographical Sciences, Fujian Normal University, Fuzhou 350007, China
2. Regional Climate Group, Department of Earth Sciences, University of Gothenburg, Box 460 S-405 30 Gothenburg, Sweden
3. Key Laboratory of Cenozoic Geology and Environment, Institute of Geology and Geophysics, Chinese Academy of Sciences, Beijing 100029, China
4. CAS Center for Excellence in Tibetan Plateau Earth Sciences
5. Department of Geography, University of Hong Kong, Pokfulam, Hong Kong.

[*] To whom correspondence should be addressed: Email: kfang@fjnu.edu.cn

Abstract

Understanding long-term drought variations in the past can help to evaluate ongoing and future hydroclimate change in the arid western Chinese Loess Plateau (WCLP), a region with increasing demand for water resources due to the increasing population and socioeconomic activities. Here we present a new tree-ring chronology inform the WCLP, which shows coherent interannual variations with tree-ring chronologies from 7 neighboring areas across the WCLP, suggesting a common regional climate control over tree growth. However, considerable differences are observed among their interdecadal variations, which are likely due to growth disturbances at interdecadal timescales. To deal with this issue, we use a frequency based method to develop a composite tree-ring chronology from 401 tree-ring series from these 8 sites, which shows more pronounced interdecadal variability than a chronology developed using traditional methods. The composite tree-ring chronology is used to reconstruct the annual precipitation from previous August to current July from 1568 to 2012, extending about 50 years longer than the previous longest tree-ring reconstruction from the region. The driest epoch of our reconstruction is found in the 1920s-30s, which matches well with droughts recorded in historical documents. Over the past four centuries, a strong resemblance between drought variability in the WCLP and western North America (WNA) is evident on multidecadal timescales, but this relationship breaks down on timescales shorter than about 50 years.

Key words: Tree ring; drought; western Chinese Loess Plateau; western North America; multi-decadal timescale

1 Introduction

Hydroclimate in the western Chinese Loess Plateau (WCLP), a boundary region of the Asian summer monsoon, is sensitive to large-scale climate anomalies (Chen et al., 2014). In this arid to semi-arid region, water availability is the major limiting factor for ecological protection, agricultural and industrial activities. Thus, improved understanding of hydroclimate regimes in the WCLP will not only add new knowledge to climate science, but also provide means to better plan future development in a sustainable way (Ren and Walker, 1998). However, the lack of instrumental data in the WCLP before the 1950s limits our ability to place recent hydroclimate conditions in a long term context. As a result, hydroclimate variations at long timescales, e.g. multi-decadal, are difficult to examine using instrumental data.

The shortness of the instrumental records can be alleviated by employing climate proxies such as tree rings to extend the observations back in time (Fritts, 1976). Although many tree-ring based reconstructions have been developed with the aim to understand hydroclimate changes in the WCLP and surroundings (Fang et al., 2010; Gou et al., 2015; Hughes et al., 1994; Kang et al., 2012; Li et al., 2007; Liang et al., 2006; Liu et al., 2008; Shao and Wu, 1994; Yang et al., 2012), the lengths of the reconstructions seldom exceed 400 years, and the spatial coverage can be improved.

In this study, we collected new tree-ring samples in Weiyuan county of the Gansu province in the WCLP to improve the temporal and spatial coverage of tree-ring data in the region. Also, by combining both new and previously published data we generated an improved and extended annual precipitation reconstruction for the entire WCLP. For the reconstruction to express regionally coherent variability, we introduced a frequency-based method to generate a composite chronology, which was expected to have better performance in retaining interdecadal climate information than when traditional methods are used. Finally, we investigated linkages between hydroclimate reconstructions in the WCLP and climate sensitive tree-ring chronologies from eastern Asia and North America to put the new reconstruction into the perspective of large-scale hydroclimate teleconnections.

2 Data and methods

2.1 Tree-ring data

The southwestern part of the WCLP is a transitional area from the Chinese Loess Plateau to world's highest plateau, the Tibetan Plateau (Figure 1), and tree-ring samples were collected in the Dieshan and Songmingyan Mountains (Fang et al., 2015). The southeastern part of the WCLP also includes the western part of the Qinling Mountain, a geographic boundary separating southern and northern China. Precipitation associated with the Asian summer monsoon allows a dominance of broadleaf forests (Figure 1). Conifers are often found on mountain peaks or cliff areas with very shallow soils (Fang et al., 2015). Precipitation decreases sharply from the southwestern and southeastern parts to the core regions of the WCLP which is dominated by loess sediments and the Gobi desert. Old growth forests in the study region are mainly found in mountains with exposed bedrock, but rarely on the commonly distributed loess mountains, likely because the bedrock provides a higher ability to retain moisture than the porous loess sediments (Fang et al., 2012). These mountains are known as "green islands" in this region, and tree-ring material has previously been collected from the Helan, Xinglong, Guiqing and Kongtong Mountains (Fang et al., 2015; Li et al., 2007), as well as the Shouyang Mountain and the Diaoling Temple sites presented in this study (Figure 1).

The Shouyang Mountain (35.03 ^{o}N, 104.32 ^{o}E) and Diaoling Temple (35.1^{o}N, 104.17^{o}E) sites are located near the Lianfeng and Qingyuan village of the Weiyuan county, respectively. Both sites only have a few old-growth trees surrounding the temples which were sampled. We took 9 increment cores from 4 old *Pinus tabulaeformis* trees at Shouyang Mountain and 22 cores from 11 old *Pinus tabulaeformis* trees at Diaoling Temple site. It should be noted that trees near temples are likely influenced by human activities. For example, it is known that local people ocassionally collected snow from the surroundings to place under the trees in winter and watered trees in summer to avoid drought stress. Unfortunately, old growth trees suitable for climate reconstruction in this area can mostly be found near the temples, since they are protected from logging due to the religious purposes. Even so, these tree-ring series are still found to be quite sensitive to climate as indicated by the significant climate-growth correlations shown below. These samples were mounted, air dried and polished following standard dendrochronological methods (Stokes and Smiley, 1968), and then crossdated by checking the matching patterns of extremely narrow and wide rings. The crossdated samples were measured and the quality of the crossdating was checked using the program COFECHA (Holmes, 1983). In addition, we found that the crossdated tree-ring width series from Shouyang Mountain and Diaoling Temple were significantly correlated with previously published tree-ring series from neighboring sites (Fang et al., 2015; Li et al., 2007). Overall, 401 of the total 603 tree-ring series from the region could be crossdated. The moderate ratio of selected vs. available tree-ring series being useful for the chronology development was largely because of the large distances among these sites. Also, to maintain the robustness of the composite chronology, only the tree-ring series that were highly correlated ($r>0.5$, $p<0.001$) were selected. This strict selection criterion excluded many tree-ring series. The selected tree-ring series included 15 out of the 31 cores from our sampling sites, 42 out of the 107 cores from Helan Mountain, 123 out of the 200 cores from Xinglong Mountain, 30 out of the 43 cores from Guiqing Mountain, 30 out of the 70 cores from Xiaolong Mountain, 45 out of the 52 cores from Kongtong Mountain, 99 out of the 101 cores from Dieshan Mountain and 17 out of the 30 cores from Songmingyan Mountain (Figure 1). Chronologies of individual sites developed from selected tree-ring series match with each other better than the chronologies developed from all series as indicated by the relatively higher correlations among the chronologies of individual sites using selected series (Figure

S1). In addition, we identified a missing ring in 1770 for all tree-ring cores from the Guiqing and Xiaolong Mountains. This missing ring had not been identified previously because of insufficient number of long tree-ring series extending beyond 1770 at these sites.

2.3 Methods

The 8 individual site tree-ring chronologies were developed using a traditional method, and composite WCLP tree-ring chronologies, based on the selected series from all the sites, were developed using two different methods: a traditional and a new frequency-based method. In the traditional method, all tree-ring series at the individual sites were fitted by a smoothed cubic spline curve with a 50% frequency cutoff of 180 years, which is equal to the mean length of the all the series, to remove the age-related growth trends. The detrended tree-ring indices were averaged following a biweight robust mean methodology to produce a chronology (Cook, 1985). The reliable portion of the tree-ring chronologies was determined when the statistic of the subsample signal strength (SSS) is higher than 0.85 (Wigley et al., 1984). The composite chronology based on the traditional method is henceforth referred to as standard.

The frequency-based method for the composite chronology development was designed to better retain interdecadal climate information by dampening the site-specific, non-climatic influences on these interdecadal timescales. We employed a

10 point butterworth filter (Ghil et al., 2002; Mann et al., 2009) to decompose the tree-ring indices into interannual (f>0.1) and interdecadal (f<0.1) variations. This filter has advantages in simulating the passband due to its quite flat frequency response in the passband (Ghil et al., 2002; Mann et al., 2009). The interannual variations generally matched well, which were thus averaged to highlight the common interannual variations of the chronology using the biweight robust mean method (Cook, 1985). We found that some interdecadal variations of tree-ring series were common across the sites while others differed (detailed below). These differing interdecadal variations are likely caused by non-climatic factors (Björklund et al., 2013). To enhance the common interdecadal climate signal, the composite chronology was developed by using only those chronologies with well-matched interdecadal variations. Herein, to define the tree rings with coherent variations, we selected those having high loadings (>0.5) on the first principal component, representing their common interdecadal variations, based on all the data.

In order to take advantage of the long tree-ring series, we employed a nested approach (Cook et al., 2002) by iteratively stepwise identifying the series with common interdecadal variations from the most replicated common period to the longest period at a step of 25 years. All of the nested chronologies were standardized to have equal mean and variance in the most replicated common period and then averaged. The final composite chronology was developed by merging the interannual and interdecadal chronologies. This frequency based method was designed to deal with the site-specific, non-climatic variations at interdecadal timescale, and differs from the previous Hilbert-Huang Transform (HHT) based method that aims to remove the tree-specific non-climatic variations of tree growths at a site (Fang et al., 2013).

Monthly temperature and precipitation data were obtained from the meteorological stations at Lintao, Minxian, Lanzhou, Tianshui, Pingliang and Yinchuan, which are located close to the tree-ring sites (see Figure 1). The instrumental data started in 1951 when most of the stations were established. The monthly climate data from these stations were averaged and the climate-growth relationships were analyzed from the start of the previous growing season (May) to the end of the current growing season in October (Fang et al., 2015). To identify the strongest climate-growth relationships, we calculated the correlations between tree growth and all possible combinations of monthly total precipitation and mean temperature, which resulted in 444 climate variables. The robustness of the reconstruction was tested using a split calibration and verification procedure (Meko and Graybill, 1995) by calibrating the tree rings using instrumental data from 1951-1981 and from 1982-2012, which were verified using the rest of data from 1982-2012 and 1951-1981, respectively. The statistics of sign test (ST), reduction of error (RE) and coefficient of efficiency (CE) were used to examine the robustness of the reconstruction, where RE and CE values greater than zero indicate acceptable reconstruction ability (Cook et al., 2010). To further validate the reconstruction, we used a set of drought reconstructions based on historical documents (Zhang et al., 2003) from 12 counties surrounding the tree-ring sites in the

WCLP, including Shanba, Etuoke, Zhangye, Yulin, Yinchuan, Xining, Yan'an, Lanzhou, Pingliang, Tianshui, Xi'an, Hanzhong (Figure 1) as independent data. This historical drought atlas classified drought into five categories from 1 to 5 to representing extremely wet, moderately wet, normal, moderately dry and extremely dry conditions, respectively. The documents based drought reconstructions start in 1470 and contain some missing values in the early periods due to insufficient historical records. We calculated the mean of these drought reconstructions from historical documents to represent the regional drought variations.

3 Results

3.1 A composite WCLP tree-ring chronology

The interannual and interdecadal variations of the 8 tree-ring width chronologies in the study are shown in Figure 2. The interannual variations are highly correlated among the sites (Figure 2a). However, there are conspicuous mismatches of interdecadal variations among these chronologies, particularly in the 1820s-1850s and the 1850s-1870s (Figure 2b). Both the mean correlations (r=0.72) and effective freedom (126.7) based on the Chelton methods (Pyper and Peterman, 1998) are higher for the correlations among the interannual variations than those for the interdecadal variations (r=0.63, effective freedom=33.2). High correlations on the interannual timescale indicate a common forcing on tree growth in the region. The differences in interdecadal growth variability among the sites, however, are likely caused by site-specific non-climatic factors and consequently need to be minimized when developing a regional composite chronology. Similar features have been found for the paired correlations among individual tree-ring chronologies of the 8 areas with more significant correlation among the high-passed (f>0.1) chronologies than the low-passed data (Table S2). Although there are paired chronologies with moderate correlations, the composite chronology were developed based only on those highly correlated tree-ring series as indicated above. It is unlikely that climate regimes differ among these neighboring sites on interdecadal timescales for this area with its coherent interannual climate patterns, because the interdecadal climate regimes often varies over large spatial areas. Moreover, at each site the tree-ring series displayed common interdecadal variations, further supporting that mismatches among interdecadal variations are not related to climate.

We generated one high-frequency mean chronology based on all the 401 tree-ring width data with coherent variations (Figure 3a) and one low-frequency mean chronology from 131 tree-ring series displaying coherent interdecadal variations (Figure 3b). The frequency based composite chronology has enhanced interdecadal variability (Figure 3c). The enhancement on the interdecadal variability is not very pronounced likely related to the close interannual variability that “blurred” the interdecadal variability. As shown in Figure 4, the frequency based chronology developed from the selected tree-ring series with coherent interdecadal variations showed stronger interdecadal variability than the standard chronology based on all the tree-ring series including some series with divergent interdecadal variations.

The interdecadal variations of the tree-ring chronology agree well with those from the drought reconstruction based on historical documents (Figure 4). Good matches between moisture sensitive tree rings and historical documents in this area have been revealed in previous studies (Liang et al., 2006; Yang et al., 2014a; Yang et al., 2014b), validating our use of tree rings for hydroclimate reconstruction in the following section. Mismatches between the two types of records are mainly observed before 1640, which may be due to the relatively few historical documents and low number of the tree-ring series included in the frequency based composite chronology in these early periods. Previous comparisons between tree rings and historical documents also indicated mismatches in these early periods (Yang et al., 2014a). The reliable portion of the composite chronology, based on an EPS value greater than 0.85 is from 1568 to 2012 (Figure 3c), which is about 50 years longer than the previously published longest chronology from the WCLP region (Fang et al., 2012).

3.2 Precipitation reconstruction of WCLP

The composite WCLP chronology show positive correlations with precipitation and negative correlations with temperature in previous and current growing seasons (Figure 5). Tree growth shows highest correlations with precipitation of a hydrological year starting in August prior to growth and ending in July of the growth year (r=0.66) (Figure 5), thus integrating precipitation signals over two years. Similar responses to hydroclimate (or precipitation) have also been found in trees growing in arid regions near the Tibetan Plateau (Fang et al., 2015).

The previous August to current July WCLP precipitation reconstruction, based on the composite chronology, explains 43.1% of the instrumental variance (Figure 6). The correspondence between the reconstructed and observed precipitation is given in Figure 6a. The ST for both tests are significant ($p<0.01$), and the RE and CE for both tests are 0.45 and 0.36 respectively, indicating acceptable reconstruction skill. We identified extreme dry (<2SD) years in 1770, 1796, 1831, 1928, 1929 and 1932 (Figure 6b), and extremely dry epochs, defined as at least 5 persistently dry (<1SD) years from the low-passed ($f<0.1$) data, during 1702-1707, 1716-1724, 1734-1737, 1827-1833, 1862-1866, and 1925-1933. The dry epoch from 1925-1933 was the most severe during the last four centuries, with 3 extremely dry years falling within this period. Extremely wet years (>2SD) were found in 1603-1607, 1751, 1753, 1755, 1786, 1803-1805, 1807, 1977, 1979 and 1980. Wet epochs were found in 1601-1610, 1750-1756, 1783-1792, 1801-1808, 1853-1857, 1963-1967 and 1976-1981. Many of the reconstructed extreme dry/wet years or periods have previously been revealed by independent tree-ring data in the WCLP and its surroundings (Gou et al., 2015; Kang et al., 2014; Kang et al., 2012; Liang et al., 2006; Yang et al., 2012). Our reconstruction also shows similar variations as the mean of the gridded reconstruction in the study region (averaged over 102 ^{o}E-108 ^{o}E; 35 ^{o}E-40 ^{o}E) from the Monsoonal Asia Drought Atlas (Cook et al., 2010) (Figure S2). However, our reconstruction shows stronger interdecadal variability than the one from the Monsoonal Asia

Drought Atlas, which is consistent with above results of the enhanced interdecadal variability of the tree-ring chronology using the new method.

4 Discussion

4.1 Influences of non-climatic factors on interdecadal variations of tree rings

It is generally believed that the influences of non-climatic factors on individual tree-ring series can be cancelled out when developing a tree-ring chronology by averaging numerous tree-ring series at a site, assuming that the common variation in tree growth is climate related (Fritts, 1976). Our study highlights that interdecadal variations caused by non-climatic factors are less likely to be averaged out during the chronology development process than interannual variations. This may largely be because non-climatic disturbances often affect similar number of biases at growth at interdecadal and interannual scales while the number of interdecadal variations is much lower than the interannual variations, causing higher ratio of biases at interannual scale than at interannual scale. An example of a non-climate related disturbances is a growth release episode of 20 years which is observed in a tree-ring series of 100 years: it can cause the ratio of biased growth of 1% at the interannual timescale but can cause the ratio of biased growth of 20% at the interdecadal timescale.

Non-climatic factors causing different interdecadal variations among sites can be human-related activities and/or natural processes. For example, enhanced tourism activities at many sites in the WCLP may have caused growth suppressions of some old trees near the temples. Logging activities can cause growth release of neighboring trees (Björklund et al., 2013; Latham and Tappeiner, 2002; Martín-Benito et al., 2010). The natural ecological processes causing different interdecadal tree-ring variations can be related to growth suppression or release due to completion from neighboring trees. The commonly used crossdating method ensures the match of high-frequency variations of tree rings, but cannot guarantee matches of the interdecadal variations. Accordingly, our frequency based method identified the sites with similar climate patterns, as indicated by coherent interannual variations, and then only the tree-ring series with coherent interdecaldal variations across sites were used to develop the final composite chronology.

It is common in dendroclimatology to compare regional tree-ring based climate reconstructions with reconstructions in surrounding regions to explore any climatic linkages. However, such comparisons often find temporally varying associations on interdecadal timescales. Our study suggests that such mismatches at interdecadal timescale could partly be caused by different non-climatic factors. The frequency based method can enhance the climate signal for a large region at interdecadal timescale, facilitating investigations of climate linkages across regions. As shown in Figure S3, the frequency-based chronology has good ability in retaining the regional climate signals at interdecadal scale. Still, it should be kept in mind that local climate signals might be dampened by merging tree-ring data across sites, if there is a low number of tree-ring series with coherent interdecadal variations with the regional chronology. For example, the local climate signals of the Helan Mountain area were not well retained because only a few tree-ring series from that region were included in the regional chronology. To test whether local climate signals are removed or not, independent proxy data, such as historical documents, should be used.

4.2 Droughts in the WCLP

Instrumental records and paleoclimate reconstructions have previously revealed similar precipitation regimes between the WCLP and northeastern Asia (Fang et al., 2012; Li et al., 2009; Pederson et al., 2001). Such co-variability is reasonable, as these regions are situated in the marginal areas of Asian summer monsoon. For example, the timing of the two most severe reconstructed droughts in our study region in the 1920s-1930s and the 1720s-1730s agrees with droughts in northeastern China and eastern Mongolia (Fang et al., 2010; Li et al., 2009; Liang et al., 2006; Pederson et al., 2001). Some dry events were likely caused by weakening of the Asian summer monsoon. For example, one of the driest years in the WCLP was found in 1796, which corresponds to a severe El Niño year (Grove, 2007). El Niño episodes are associated with colder-than-normal western equatorial Pacific Ocean, and thus reduced convective activities, which can weaken the Asian summer monsoon and thus cause dry condition in its front regions (Ju and Slingo, 1995).

Although drought variations in the WCLP have consistencies with those in other marginal monsoon areas, the degrees of dryness in these marginal areas can be different. Based on our drought reconstruction for the entire WCLP, the driest period during the past four centuries was in 1925-1933. This drought, which has been widely described in historical documents, was observed in over 20 provinces in China (Li, 1994; Liang et al., 2006), as well as inferred from stalagmite records in the WCLP (Zhang et al., 2008) and tree-ring data from northeastern and central Mongolia (Pederson et al., 2001). Between 1928 and 1933, the drought induced serious reduction in food productivity causing a famine that killed about 2.5 to 3 million people, which was about half of the population in the Gansu province covering most of our study region (Li, 1994).

Other studies have suggested that the drought in the 1630s-1640s, which may have contributed to the fall of the Chinese Ming Dynasty, was the severest during the past four centuries in the marginal areas of the Asian summer monsoon (Cook et al., 2010; Zhang et al., 2008). However, according to our reconstruction, this period was only moderately dry in the WCLP (Figure 6). This is likely because the 1920s-1930s drought was centered over the WCLP, while the 1630s-1640s drought was centered over northeastern China (Cook et al., 2010; Li, 1994; Zhang et al., 2008). Another dry period that had its core area in northeastern China, but still affecting the WCLP, was the “Great Victorian Drought” from 1876-1878, which has been recorded in both tree-ring data (Cook et al., 2010) and historical documents (Li, 1994). Regional differences among these extended droughts suggest that the dynamics of the Asian summer monsoon is spatially variable in its boundary regions, with droughts of different magnitude centered in different sub-regions.

4.3 Co-varying climate changes in the WCLP and western North America (WNA)

Compared to other paleoclimate proxies, tree-ring data have advantages to facilitate investigations of large-scale climate changes due to their large and dense spatial coverage (Fritts, 1976). To explore the linkages with large-scale climate patterns, we compared our WCLP reconstruction with other climate sensitive tree-ring chronologies (Table S1) from Eastern Asia and North America (Figure 7), as hydroclimate changes in this pan-Pacific area haven been revealed to be closely linked (Fang et al., 2016). The tree-ring chronologies were mainly derived from the drought Atlas in Asia and North America (Cook et al., 2010; Cook et al., 2004) and the PAGES 2k dataset (PAGES 2k Consortium, 2013). Our composite chronology shows significant correlations at multi-decadal scales with other tree-ring chronologies in distant regions, particularly in WNA(Figure 7a and 7b). On the interannual timescales, high correlations are only obtained with tree-ring chronologies in neighboring regions (Figure 7c and 7d). There may be different controlling factors for regional precipitation at different timescales. Locally consistent variations in tree rings in the neighboring areas may suggest the dominance of local surface conditions, such as vegetation cover and topographic features, which can modulate the local water cycles through, for example, the soil moisture content, evaporation, convection and nuclei formations (Huang et al., 2015). On the other hand, co-variability of multi-decadal precipitation variability across remote regions indicates that large-scale circulation pattern play a larger role at these timescale. This is because large-scale oceanic and atmospheric patterns are more likely to cause concurrent climate anomalies in distant regions through teleconnections compared to local water cycles (Li et al., 2013; Ortega et al., 2015). In addition, the WCLP-WNA hydroclimate linkages are likely part of the large-scale climate linkages between eastern Asia and North America (Figure S4). The WCLP and WNA appear to among the key regions showing close linkages between climate changes in eastern Asia and North America over the past 4 centuries (Figure S4).

This study highlights the timescale dependency of climate regimes, which can vary when certain threshold timescale is crossed. For example, climate change between our study region and WNA has almost no linkage (Figure 8a) on interannual timescale, but they have close matches at multi-decadal timescales (Figure 8b). The WCLP-WNA co-variability sharply becomes significant at a threshold timescale of ~ 50 years, suggesting that the controlling climate factors on this co-variability have periodicities over ~50 years. We thus investigate the possible causes of the linkages between our reconstruction and climate in WNA at multi-decadal timescale only.

To further test whether our reconstruction reveals large-scale climate patterns, we compared our reconstruction with reconstructions of large-scale climate patterns. At multi-decadal timescale, the Pacific climate is largely modulated by the Pacific

Decadal Oscillation (PDO) (Mantua and Hare, 2002), which is considered as the norther part of the Interdecadal Pacific Oscillation (IPO) (Henley et al., 2015). However, the existing PDO reconstructions have considerable mismatches among each other, which provided different depending on PDO reconstructions used (Kipfmueller et al., 2012). We thus employed an IPO reconstruction based on tree-ring data of the Pacific area that revealed coherent interdecadal climate patterns over the entire Pacific Ocean area (Fang et al., 2016). The IPO is also documented to have a strong impact on global climate at multi-decadal/interdecadal timescale (Dai et al., 2015; Kosaka and Xie, 2013). Apart from IPO, the Atlantic Multi-decadal Oscillation (AMO) has been widely recognized to have strong modulation on multi-decadal climate variability across the globe (Schlesinger and Ramankutty, 1994; Sonechkin et al., 1999). Proxies from both the Atlantic and Pacific regions have revealed AMO signals (Gray et al., 2004; Wang et al., 2011). The AMO reconstructions are robust at multi-decadal timescale since the reconstructions using proxies from independent sources in Atlantic and Pacific regions have similar multi-decadal variability. We thus employed an AMO reconstruction by Gray et al. (2004) based on proxies from Atlantic regions. As shown in Figure 8c, our reconstruction agrees well with the IPO reconstruction, where almost all cycles match. This suggests that the multi-decadal variability of the WCLP is modulated by the IPO and our study region is one of the key regions linked to IPO variability. However, how IPO modulates regional climate, and thus tree-ring growths, is still uncertain because the shortness of the instrumental data for this region. Our results suggest that there is a possibility that the IPO modulates multi-decadal temperature and/or precipitation to cause regional multi-decadal climate change.

5 Conclusions

Our newly developed tree-ring series at Shouyang Mountain and Diaoling Temple sites are highly correlated at interannual timescale with most of the moisture sensitive tree-ring series from 7 surrounding areas in the WCLP, suggesting a common precipitation regime in the region. However, mismatches were observed of the interdecadal variations among the tree-ring data in the region, which are likely caused by local non-climatic disturbances. This study highlights that non-climatic disturbances at interdecadal timescale are less likely to be averaged out during the chronology development process relative to disturbances at interannual timescale. To enhance the common climate signal also on interdecadal timescales, we used a frequency based method to develop the regional composite chronology which only included tree-ring series with coherent interdecadal variations across sites.

We used 401 tree-ring series to develop a composite chronology for the WCLP spanning from 1568 to 2012, which is about 50 years longer than the previously published one. The frequency based tree-ring chronology showed stronger interdecadal variations than the chronology built using traditional methods. It was used to reconstruct the annual precipitation from previous August to current July back to 1568, whiere the reconstruction explained 43.1% of the instrumental variance.

Interdecadal drought variations revealed in this tree-ring based reconstruction agree well with the drought histories recorded in historical documents. Reconstructed precipitation variability in the WCLP was very similar to the drought variability in the WNA at multi-decadal ($f<0.02$) timescales, while no linkage was found in the higher frequencies. This linkage at multi-decadal timescales is likely due to the common influences of the IPO on hydroclimate in the two regions.

Acknowledgements: We thank Jiang Chen, Yajun Chen, Qiuyan Chen, Dan Chen and Wanying Xu for their helps in the field and the lab. This research was funded by the National Basic Research Program of China (973) (2012CB955301), National Science Foundation of China (41471172, 41690114 and U1405231), the Fellowship for Distinguished Young Scholars of Fujian Province (2015J06008), as well as the Swedish BECC, MERGE and VR grants.

References

Björklund JA, Gunnarson BE, Krusic PJ, Grudd H, Josefsson T, Östlund L, Linderholm HW (2013) Advances towards improved low-frequency tree-ring reconstructions, using an updated Pinus sylvestris L. MXD network from the Scandinavian Mountains. Theoretical and applied climatology 113: 697-710

Chen J, Chen F, Feng S, Huang W, Liu J, Zhou A (2014) Hydroclimatic changes in

China and surroundings during the Medieval Climate Anomaly and Little Ice Age: Spatial patterns and possible mechanisms. Quaternary Science Reviews 107: 98–111

Cook E, Anchukaitis KJ, Buckley BM, D'Arrigo RD, Jacoby GC, Wright WE (2010) Asian Monsoon Failure and Megadrought During the Last Millennium. Science 328: 486-489

Cook E, Seager R, Cane MA, Stahle DW (2007) North American drought: reconstructions, causes, and consequences. Earth-Sci Rev 81: 93-134

Cook E, Woodhouse CA, Eakin CM, Meko DM, Stahle DW (2004) Long-term aridity changes in the western United States. Science 306: 1015

Cook ER (1985) A time series analysis approach to tree ring standardization. vol PhD. The University of Arizona, Tucson, USA

Cook ER, D'Arrigo RD, Mann ME (2002) A well-verified, multiproxy reconstruction of the winter North Atlantic Oscillation Index since ad 1400. Journal of Climate 15: 1754-1764

Dai A, Fyfe JC, Xie SP, Dai X (2015) Decadal Modulation of Global Surface Temperature By Internal Climate Variability. Nature Climate Change 5: DOI: 10.1038/NCLIMATE2605

Fang K, Cook E, Guo Z, Chen D, Ou T, Frank D, Zhao Y (2016) Synchronous multi-decadal tree-ring patterns of the Pacific areas reveal dynamics of the Interdecadal Pacific Oscillation (IPO) since 1567 In review

Fang K, Frank D, Gou X, Chen F, Liu C, Li J, Li Y (2013) Precipitation variations over the past four centuries in the Dieshan Mountain area inferred from tree rings: an introduction to a HHT-based method. Global and Planetary Change doi: 10.1016/j.gloplacha.2013.04.010

Fang K, Frank D, Zhao Y, Zhou F, Seppä H (2015) Moisture stress of a hydrological year on tree growth in the Tibetan Plateau and surroundings. Environmental Research Letters 10: 034010, doi:034010.031088/031748-039326/034010/034013/034010

Fang K, Gou X, Chen F, D'Arrigo R, Li J (2010) Tree-ring based drought reconstruction for the Guiqing Mountain (China): linkages to the Indian and Pacific Oceans. Int J Climatol 30: 1137-1145

Fang K, Gou X, Chen F, Liu C, Davi N, Li J, Zhao Z, Li Y (2012) Tree-ring based reconstruction of drought variability (1615–2009) in the Kongtong Mountain area, northern China. Global and Planetary Change 80-81: 190-197

Fritts HC (1976) Tree rings and climate. Academic Press, New York

Ghil M, Allen M, Dettinger M, Ide K, Kondrashov D, Mann M, Robertson AW, Saunders A, Tian Y, Varadi F (2002) Advanced spectral methods for climatic time series. Reviews of geophysics 40: 3-1-3-41

Gou X, Deng Y, Gao L, Chen F, Cook E, Yang M, Zhang F (2015) Millennium tree-ring reconstruction of drought variability in the eastern Qilian Mountains, northwest China. Climate Dynamics 45: 1761-1770

Gray ST, Graumlich LJ, Betancourt JL, Pederson GT (2004) A tree-ring based reconstruction of the Atlantic Multidecadal Oscillation since 1567 AD.

Geophysical Research Letters 31: L12205. DOI: 12210.11029/12004GL019932

Grove RH (2007) The Great El Niño of 1789–93 and its Global Consequences Reconstructing an Extreme Climate Event in World Environmental History. The Medieval History Journal 10: 75-98

Henley BJ, Gergis J, Karoly DJ, Power S, Kennedy J, Folland CK (2015) A tripole index for the interdecadal Pacific oscillation. Climate Dynamics 45: 3077-3090

Hoerling M, Kumar A (2003) The perfect ocean for drought. Science 299: 691-694

Holmes RL (1983) Computer-assisted quality control in tree-ring dating and measurement. Tree-ring bull 43: 69-78

Huang J, Yu H, Guan X, Wang G, Guo R (2015) Accelerated dryland expansion under climate change. Nature Climate Change

Hughes MK, Wu X, Shao X, Garfin GM (1994) A Preliminary Reconstruction of Rainfall in North-Central China since A.D. 1600 from Tree-Ring Density and Width. Quaternary Research 42: 88-99

Ju J, Slingo J (1995) The Asian summer monsoon and ENSO. Quarterly Journal of the Royal Meteorological Society 121: 1133-1168

Kang S, Bräuning A, Ge H (2014) Tree-ring based evidence of the multi-decadal climatic oscillation during the past 200 years in north-central China. Journal of Arid Environments 110: 53-59

Kang S, Yang B, Qin C (2012) Recent tree-growth reduction in north central China as a combined result of a weakened monsoon and atmospheric oscillations. Climatic Change 115: 519-536

Kipfmueller KF, Larson ER, St George S (2012) Does proxy uncertainty affect the relations inferred between the Pacific Decadal Oscillation and wildfire activity in the western United States? Geophysical Research Letters 39: DOI: 10.1029/2011GL050645

Kosaka Y, Xie S-P (2013) Recent global-warming hiatus tied to equatorial Pacific surface cooling. Nature 501: 403-407

Latham P, Tappeiner J (2002) Response of old-growth conifers to reduction in stand density in western Oregon forests. Tree Physiology 22: 137-146

Li J, Chen F, Cook ER, Gou X, Zhang Y (2007) Drought reconstruction for north central China from tree rings: the value of the Palmer drought severity index. Int J Climatol 27: 903-909

Li J, Cook ER, Chen F, Davi N, D'Arrigo R, Gou X, Wright WE, Fang K, Jin L, Shi J (2009) Summer monsoon moisture variability over China and Mongolia during the past four centuries. Geophysical Research Letters 36: L22705 doi:22710.21029/22009GL041162

Li J, Xie SP, Cook E, Morales MS, Christie DA, Johnson NC, Chen F, D'Arrigo R, Fowler AM, Gou X, Fang K (2013) El Niño Modulations over the Past Seven Centuries: Amplitude, Teleconnection, and the Volcanic Effect. Nature Climate Change 3: DOI: 10.1038/NCLIMATE1936

Li W (1994) The top ten famine in recent China. Shanghai People's Press

Liang E, Liu X, Yuan Y, Qin N, Fang X, Huang L, Zhu H, Wang L, Shao X (2006) The 1920s drought recorded by tree rings and historical documents in the semi-arid and arid areas of northern China. Climatic Change 79: 403-432

Liu Y, Cai Q, Liu W, Yang Y, Sun J, Song H, Li X (2008) Monsoon precipitation variation recorded by tree-ring δ 18 O in arid Northwest China since AD 1878. Chemical Geology 252: 56-61

MacDonald GM, Case RA (2005) Variations in the Pacific Decadal Oscillation over the past millennium. Geophys Res Lett 32: L08703, doi:08710.01029/02005GL022478

Mann ME, Zhang Z, Rutherford S, Bradley RS, Hughes MK, Shindell D, Ammann C, Faluvegi G, Ni F (2009) Global signatures and dynamical origins of the Little Ice Age and Medieval Climate Anomaly. Science 326: 1256-1260

Mantua NJ, Hare SR (2002) The Pacific decadal oscillation. Journal of Oceanography 58: 35-44

Martín-Benito D, Del Río M, Heinrich I, Helle G, Cañellas I (2010) Response of climate-growth relationships and water use efficiency to thinning in a Pinus nigra afforestation. Forest Ecology and Management 259: 967-975

Meko D, Graybill DA (1995) Tree-ring reconstruction of upper Gila river discharge. J Am Water Resour As 31: 605-616

Ortega P, Lehner F, Swingedouw D, Masson-Delmotte V, Raible CC, Casado M, Yiou P (2015) A model-tested North Atlantic Oscillation reconstruction for the past millennium. Nature 523: 71-74

PAGES 2k Consortium (2013) Continental-scale temperature variability during the past two millennia. Nature Geoscience 6 339-346

Pederson N, Jacoby GC, D'Arrigo RD, Cook ER, Buckley BM, Dugarjav C, Mijiddorj R (2001) Hydrometeorological Reconstructions for Northeastern Mongolia Derived from Tree Rings: 1651-1995. J Climate 14: 872-881

Pyper BJ, Peterman RM (1998) Comparison of methods to account for autocorrelation in correlation analyses of fish data. Canadian Journal of Fisheries and Aquatic Sciences 55: 2127-2140

Ren M-e, Walker JH (1998) Environmental consequences of human activity on the Yellow River and its delta, China. Physical Geography 19: 421-432

Ruddiman W (2014) Earth's Climate: past and future. W H Freeman & Company, New York

Schlesinger ME, Ramankutty N (1994) An oscillation in the global climate system of period 65-70 years. Nature 367: 723-726

Seidel DJ, Fu Q, RanDel WJ, ReichleR TSJ (2007) Widening of the tropical belt in a changing climate. Nature Geoscience 1: 21-24

Shao X, Wu X (1994) Radial growth of Huashan Pine and its response to climate. Journal of Chinese Geography 4: 88-102

Sonechkin D, Astafyeva N, Datsenko N, Ivachtchenko N, Jakubiak B (1999) Multiscale oscillations of the global climate system as revealed by wavelet transform of observational data time series. Theoretical and applied climatology 64: 131-142

Stokes MA, Smiley TL (1968) An introduction to tree-ring dating. University of Chicago Press, Chicago, Illinois

Wang X, Brown PM, Zhang Y, Song L (2011) Imprint of the Atlantic multidecadal oscillation on tree-ring widths in Northeastern Asia since 1568. PloS one 6: e22740

Wigley TML, Briffa KR, Jones PD (1984) Average value of correlated time series, with applications in dendroclimatology and hydrometeorology. J Appl Meteorol Clim 23: 201-234

Yang B, Feng S, Sonechkin DM, Qin C (2012) Tree ring-based annual streamflow reconstruction for the Heihe River in arid northwestern China from AD 575 and its implications for water resource management. Holocene 22: 773-784

Yang B, Kang S, Ljungqvist FC, He M, Zhao Y, Qin C (2014a) Drought variability at the northern fringe of the Asian summer monsoon region over the past millennia. Climate dynamics 43: 845-859

Yang B, Qin C, Wang J, He M, Melvin TM, Osborn TJ, Briffa KR (2014b) A 3,500-year tree-ring record of annual precipitation on the northeastern Tibetan Plateau. Proceedings of the National Academy of Sciences 111: 2903-2908

Zhang D, Li X, Liang Y (2003) Complementary Data of the Yearly Charts of Dryness/Wetness in China for the Last 500 years Period. . Journal of Applied Meteorological Science 14: 379-384

Zhang P, Cheng H, Edwards RL, Chen F, Wang Y, Yang X, Liu J, Tan M, Wang X (2008) A test of climate, sun, and culture relationships from an 1810-year Chinese cave record. Science 322: 940-942

Figure Captions

Figure 1. Location of the tree-ring sites developed previously and in this study, the counties with historical drought archives, the meteorological stations in western Chinese Loess Plateau (WCLP). The inset indicating the location of the study region in eastern Asia.

Figure 2. The (a) mean running correlations between the interannual (f>0.1) and

interdecadal (f<0.1) variations of the tree-ring chronologies of the 8 areas based on a 51-year window, and the (b) visual comparisons among the interdecadal variations among these chronologies in western Chinese Loess Plateau (WCLP) during their common period from 1797 to 1999. The mean running correlations were determined by first calculating the correlations between individual tree-ring chronologies of each site and the mean of all the chronologies of 8 areas, and then the correlations for individual tree-ring chronologies were averaged to produce the mean running correlations.

Figure 3. The (a) mean of the interannual (f>0.1) variations of the tree-ring indices, the (b) mean of the interdecadal (f<0.1) variations of the tree-ring series during their common period and the (c) comparisons between the "standard chronology" and the "frequency based chronology". The standard chronology was developed using traditional methods by averaging all the crossdatable tree-ring indices, which have the age-related growth trends being removed. The frequency based chronology was produced using the introduced frequency based method, which averages the mean of the interannual and the interdecadal tree-ring series, respectively. The frequency based methods treats the tree-ring series at the interannual and interdecadal scale separately and ensures both the interannual and interdecadal tree-ring series are well matched.

Figure 4. Comparisons among the interdecadal (f<0.1) variations of the "frequency based chronology" by averaging the crossdatable tree-ring series from all sites using the frequency based method, the "documents based reconstruction" of drought using historical documents in western Chinese Loess Plateau (WCLP), and the "standard

chronology" developed calculated as the arithmetic mean of of all the tree-ring series in WCLP following traditional methods.

Figure 5. Climate-growth correlations for the (a) tree-ring chronology developed for the newly introduced tree rings at Shouyang Mountain and Diaolin Temple sites and for the (b) composite chronology developed from tree rings at all sites. The correlation coefficients with monthly temperature and precipitation were calculated from the start of the previous (-) year in May till the end of the current (+) year in October. The peak correlations with precipitation from previous August to current July is also shown.

Figure 6. The (a) comparisons between the actual and reconstructed precipitation since 1951 and the (b) drought reconstructions based on the reliable portion of the tree-ring chronology since 1568.

Figure 7. Maps of (a) correlations between the low-passed ($f<0.02$) composite tree-ring chronology in western Chinese Loess Plateau (WCLP) and the tree-ring chronologies in Asia and (b) correlations between the low-passed chronology in WCLP and North America (NA), (c) correlations between the high-passed ($f>0.1$) composite chronology and the chronologies in Asia, and the (d) correlations between the high-passed chronology in WCLP and chronologies in NA. The squares in maps indicate the correlations between tree rings in WCLP and western NA (WNA) at the multi-decadal timescale. These tree-ring chronologies derived from currently most complete tree-ring datasets derived from the Monsoonal Asia Drought Atlas and the North America Drought Atlas and the PAGES 2k Project. We only included the

tree-ring chronologies longer than 400 years. All the data are public avaible from National Climate Data Center (NCDC).

Figure 8. The (a) comparisons between the composite tree-ring chronology in western Chinese Loess Plateau (WCLP) and the mean of the tree-ring chronologies in western North America (WNA), the (b) comparisons between the multi-decadal (f<0.02) variations of the chronologies of WCLP and WNA and the (c) comparisons between the multi-decadal variations of the chronologies of WCLP and the reconstructions of the Atlantic Multi-decadal Oscillation (AMO) by Gray et al. (2004) and the Interdecadal Pacific Oscillation (IPO) by Fang et al. (2016). The IPO reconstruction was reversed (multiplying -1) to facilitating comparisons.

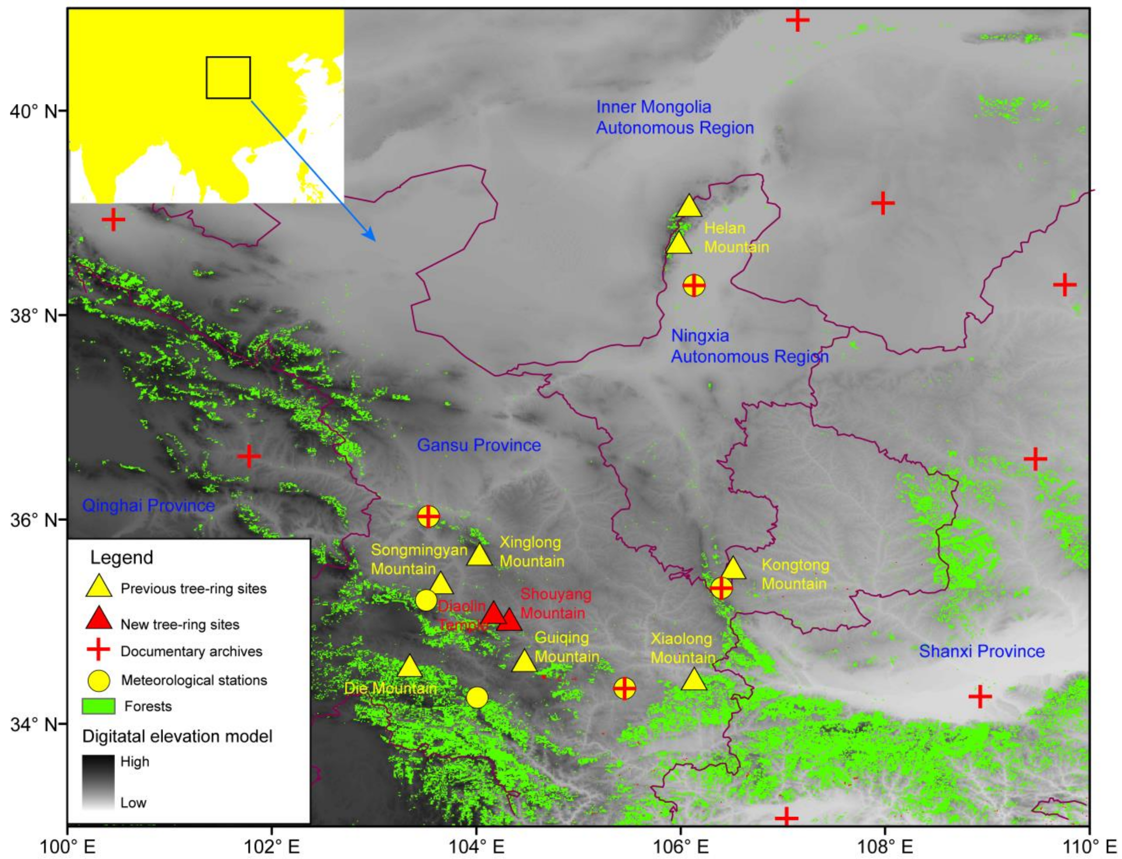

40° N
38° N
36° N
34° N
100° E
102° E
104° E
106° E
108° E
110° E
Inner Mongolia
Autonomous Region
Helan
Mountain
Ningxia
Autonomous Region
Gansu Province
Qinghai Province
Xinglong
Mountain
Songmingyan
Mountain
Shouyang
Mountain
Diaolin
Temple
Guiqing
Mountain
Xiaolong
Mountain
Kongtong
Mountain
Die Mountain
Shanxi Province
Legend
Previous tree-ring sites
New tree-ring sites
Documentary archives
Meteorological stations
Forests
Digitatal elevation model
High
Low

Figure 1.

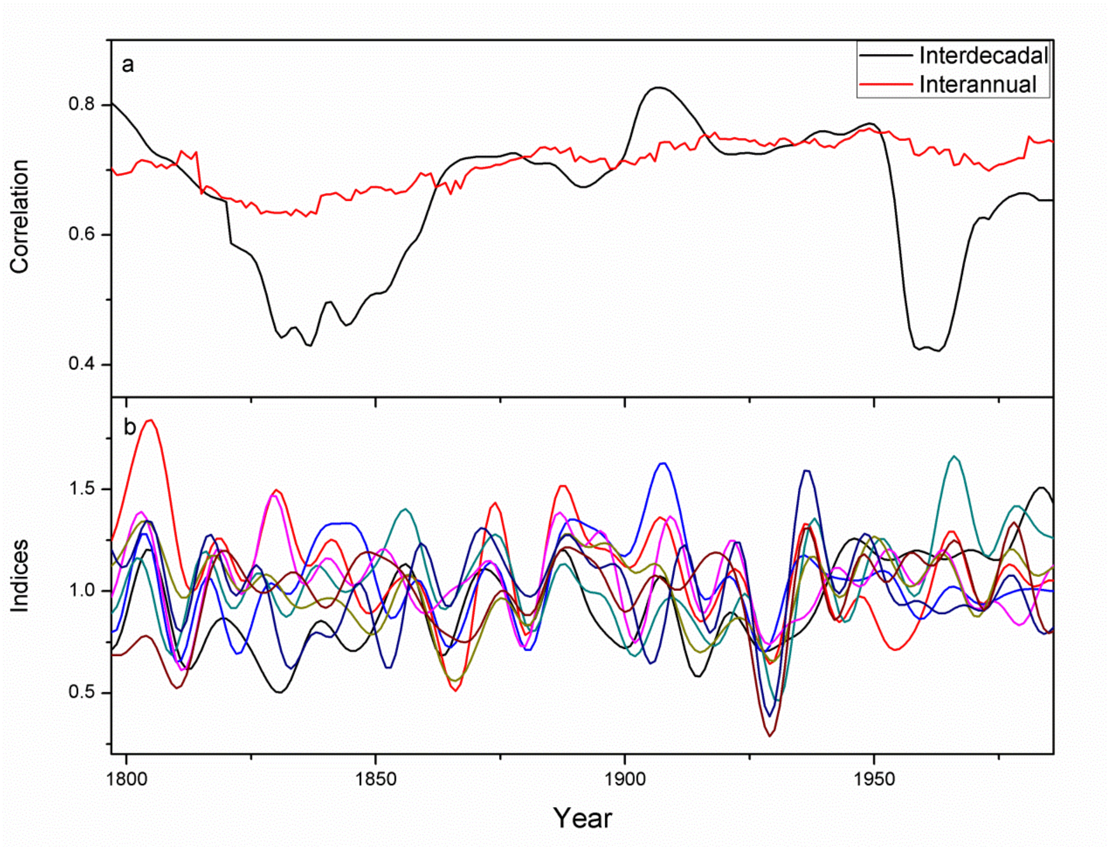
a
Interdecadal
Interannual
Correlation
0.8
0.6
0.4
b
Indices
1.5
1.0
0.5
1800
1850
1900
1950
Year

Figure 2.

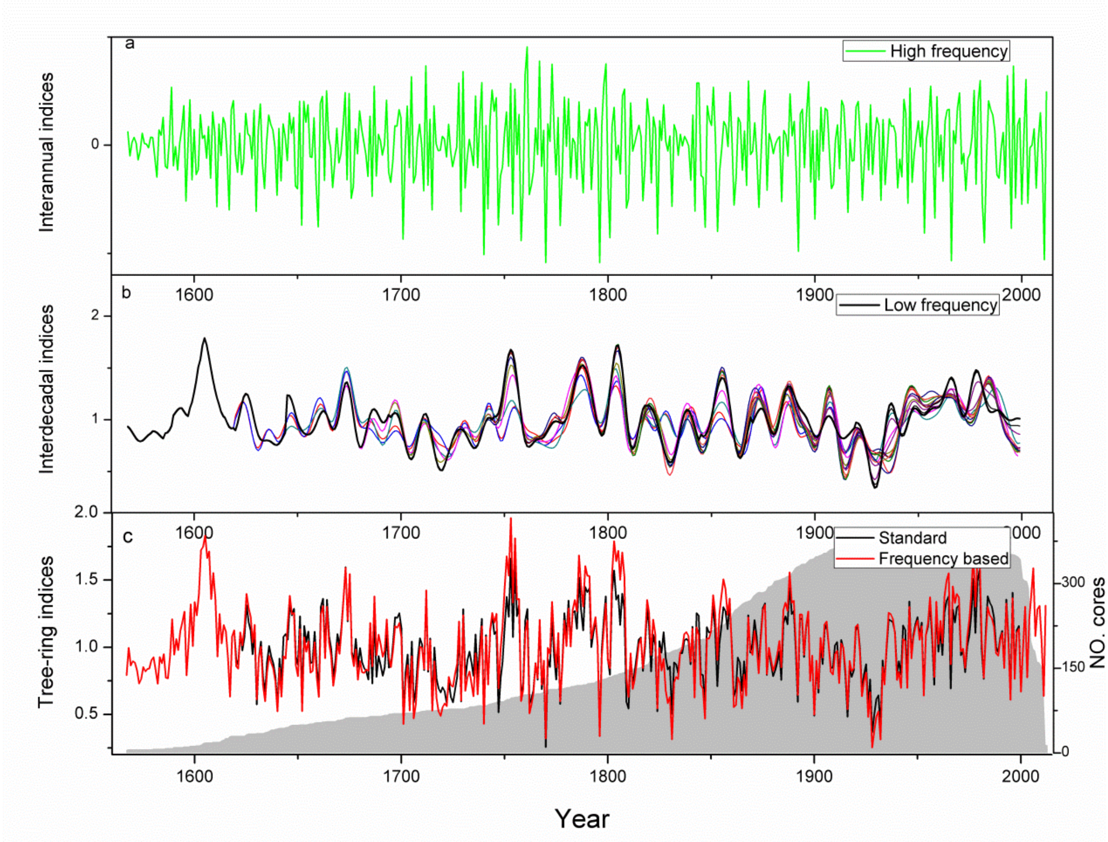
a
High frequency
Interannual indices
0
b
Low frequency
Interdecadal indices
2
1
2.0
c
Standard
Frequency based
Tree-ring indices
1.5
1.0
0.5
300
150
0
NO. cores
1600
1700
1800
1900
2000
Year

Figure 3.

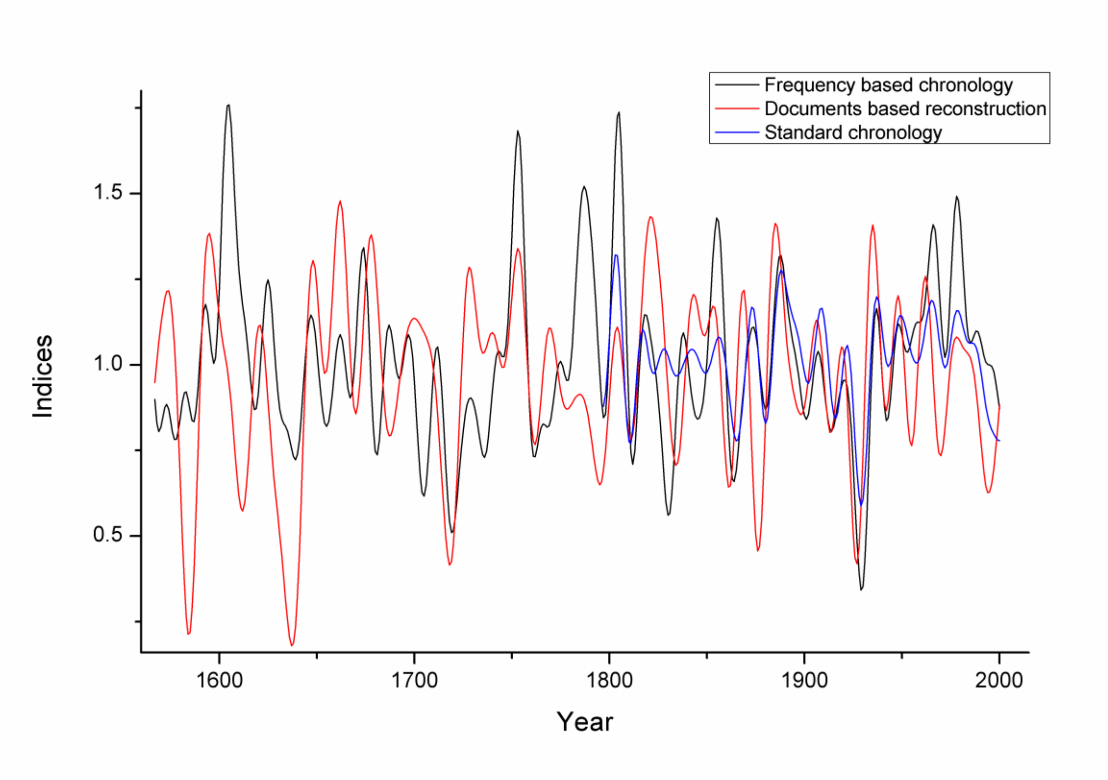
Frequency based chronology
Documents based reconstruction
Standard chronology
Indices
1.5
1.0
0.5
1600
1700
1800
1900
2000
Year

Figure 4.

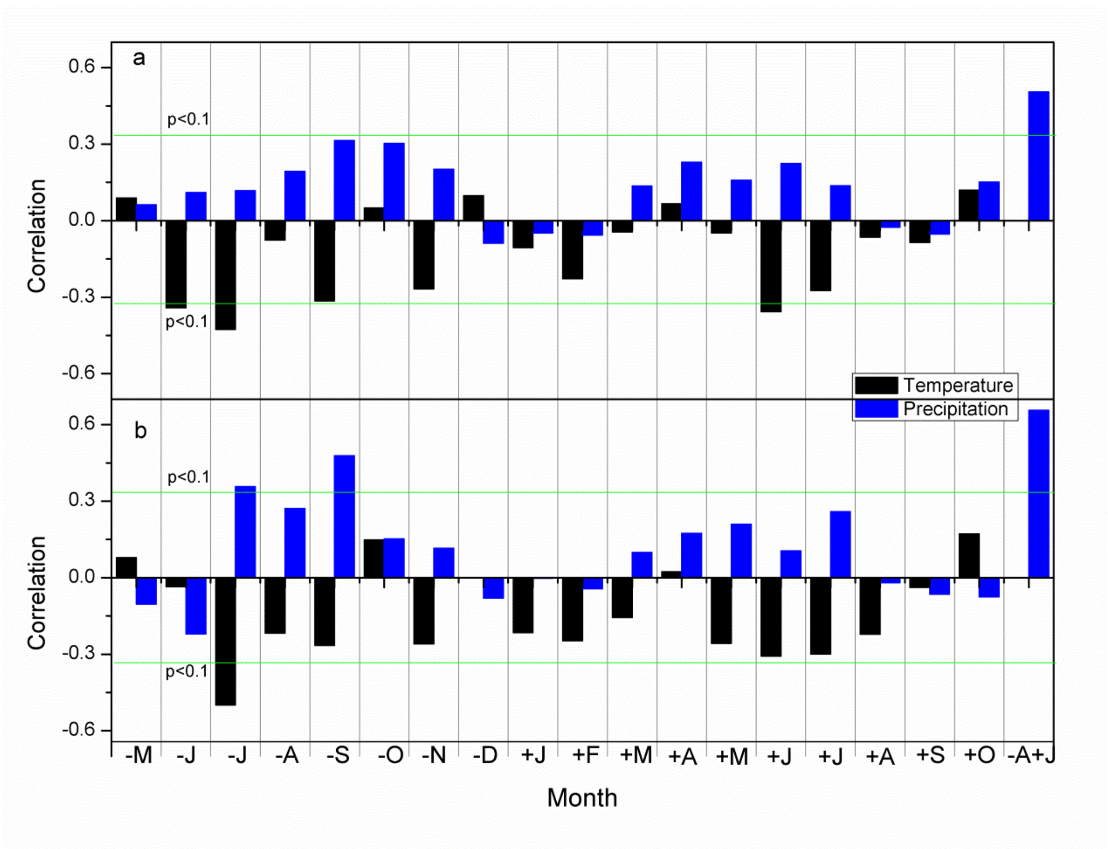
a
b
0.6
0.3
0.0
-0.3
-0.6
Correlation
p<0.1
Temperature
Precipitation
-M
-J
-J
-A
-S
-O
-N
-D
+J
+F
+M
+A
+M
+J
+J
+A
+S
+O
-A+J
Month

Figure 5.

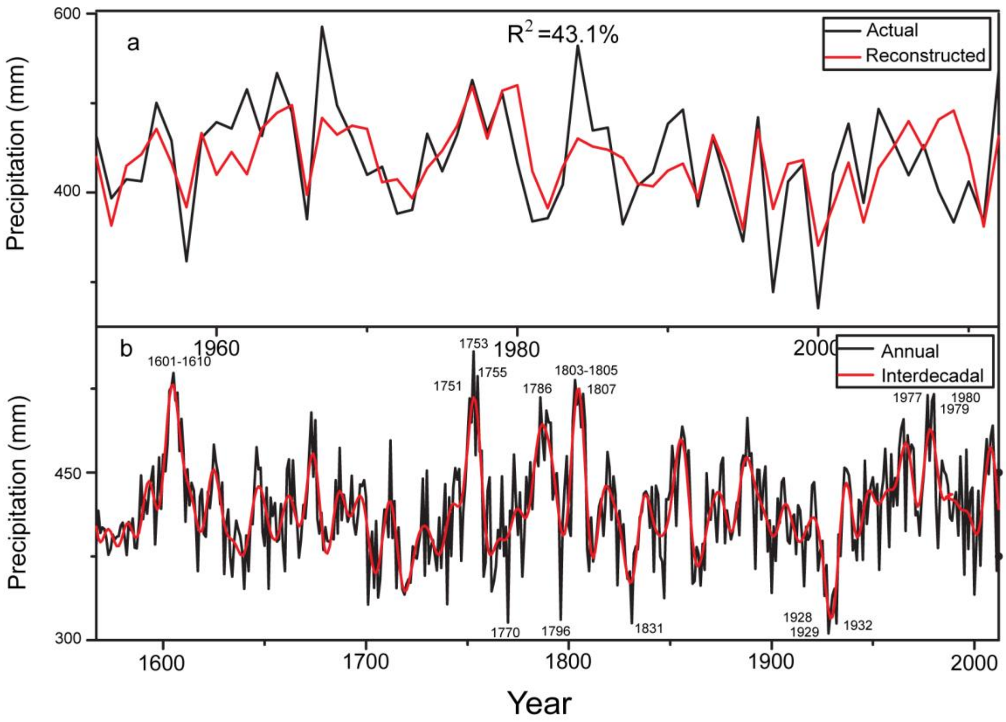
a
R^2 =43.1%
Actual
Reconstructed
Precipitation (mm)
600
400
b
1960
1980
2000
Annual
Interdecadal
1601-1610
1751
1753
1755
1770
1786
1796
1803-1805
1807
1831
1928
1929
1932
1977
1979
1980
450
300
1600
1700
1800
1900
2000
Year

Figure 6.

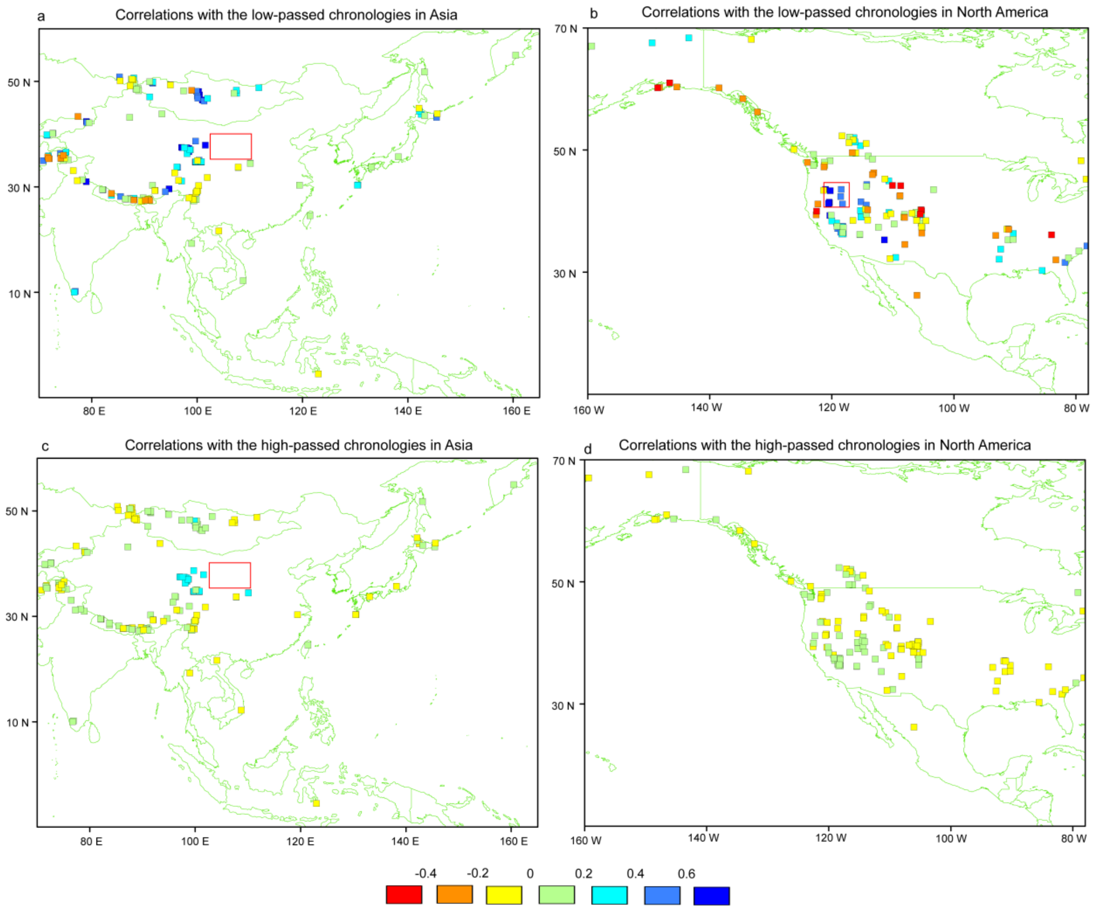
a
Correlations with the low-passed chronologies in Asia
b
Correlations with the low-passed chronologies in North America
c
Correlations with the high-passed chronologies in Asia
d
Correlations with the high-passed chronologies in North America
70 N
50 N
30 N
10 N
80 E
100 E
120 E
140 E
160 E
160 W
140 W
120 W
100 W
80 W
-0.4
-0.2
0
0.2
0.4
0.6

Figure 7.

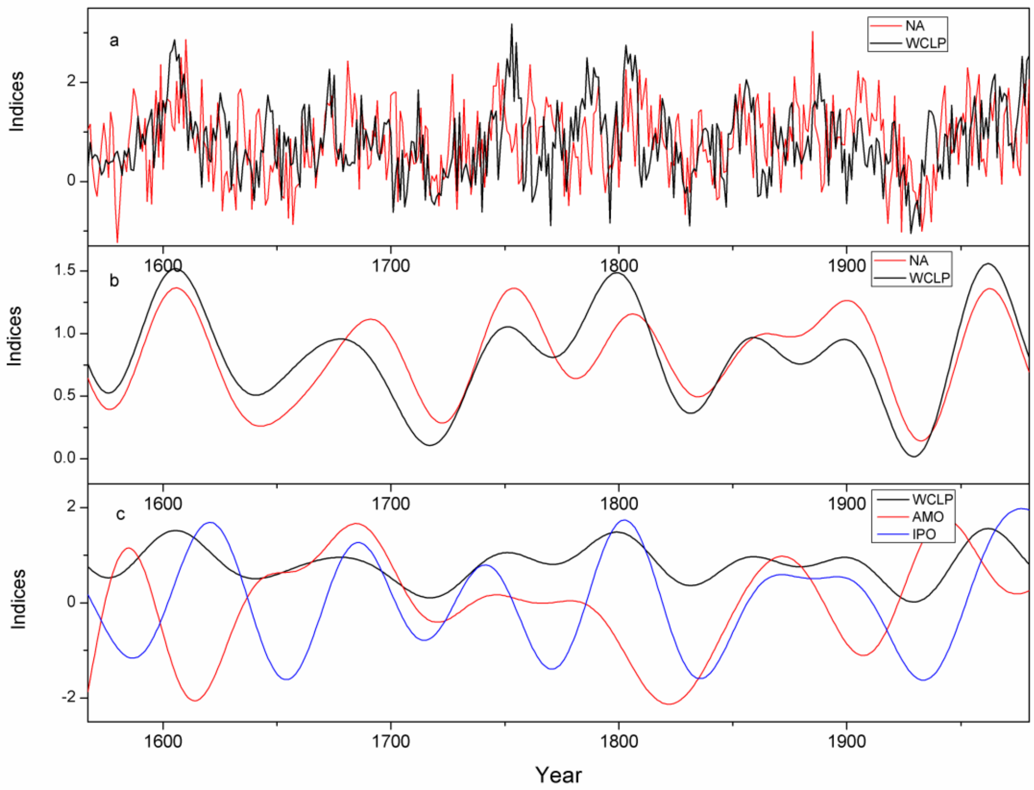
a
NA
WCLP
Indices
b
NA
WCLP
Indices
c
WCLP
AMO
IPO
Indices
1600
1700
1800
1900
Year

Figure 8.